SSRG International Journal of Mechanical Engineering
ISSN: 2348-8360/ https://doi.org/10.14445/23488360/IJME-V12I11P112

Volume 12 Issue 11, 125-134, November 2025

Original Article

Conceptual Design and Development of a Potato Peeling and Cutting Machine

Laurent Libog[1,2,3], Suzie Viviane Obame[1,2,3], Jonas Peequeur Essome Mbang[1,2,3*], Michel Mbere Taoga[1,2,3]

[1]*Department of Mechanical Engineering, ENSET, University of Douala, Douala, Cameroon.*
[2]*Groupe de Recherche sur les Matériaux Innovants (GRMI), University of Douala, Douala, Cameroon.*
[3]*Laboratory of Mechanics (LM), Postgraduate Training Unit for Engineering Sciences (UFD-SI), University of Douala, Douala, Cameroon.*

[*]*Corresponding Author : essomembangjonaspeequeur@gmail.com*

Received: 12 September 2025 Revised: 14 October 2025 Accepted: 15 November 2025 Published: 28 November 2025

Abstract *- Potato (Solanum tuberosum), a staple food in Cameroon, is widely consumed in the form of fries. However, most restaurants and fast-food outlets still rely on manual peeling and cutting, which are time-consuming, unsafe, and inefficient, particularly when customer demand is high. To overcome these limitations, this study presents the design and development of a potato peeling and cutting machine that integrates both functions into a single system. The methodology included a review of existing solutions, selection of suitable materials, component dimensioning, Computer-Aided Design (CAD), and prototype testing. The prototype (30×130×120 cm^3) achieved 95% peeling efficiency and processed 7 kg of potatoes in 7 minutes: 3 minutes for peeling and 4 minutes for cutting. This innovation provides a low-cost, locally adapted solution to the growing demand for processed potatoes in Cameroon. It can improve the productivity of Small and Medium-sized Enterprises (SMEs), reduce physical effort, and contribute to the development of the local agri-food industry.*

Keywords *- Potato, Fries, Peeling, Cutting, Prototype.*

1. Introduction

The potato (Solanum tuberosum), native to South America [1], is today one of the most widely consumed tubers worldwide. Introduced in Europe under the name patata [2], it is now cultivated in tropical regions and valued for its richness in vitamins and minerals [3]. Beyond its nutritional role, it is used in cosmetics, bakery, and especially in catering [4]. More than one billion people consume potatoes daily, making them a staple food crop on a global scale [5].

Transforming potatoes into parallelepiped-shaped fries allows the production of a semi-finished product that is highly demanded in the food sector. This also valorizes surplus harvests that cannot be sold fresh, facilitating storage and distribution to consumers [6]. Globally, and in Cameroon in particular, the consumption of fried potatoes is steadily increasing.

In Cameroon, the annual production of potatoes fluctuates between 220,000 and 400,000 tons [4]. Figure 1 illustrates the evolution of potato production between 2015 and 2022. Despite this availability, restaurants and fast-food outlets face difficulties meeting high demand, as peeling and cutting are still mostly performed manually.

Several devices already exist to mechanize peeling and cutting (Figure 2). The manual potato cutter (Figure 2(a)) requires significant physical effort, and its exposed blade poses safety risks for the operator [7]. The hand-cranked machine (Figure 2(b)) reduces effort but remains bulky and costly [7]. The semi-automatic peeler-cutter (Figure 2(c)) combines peeling and cutting but is energy-intensive due to the use of two motors and is primarily designed for large-scale industrial production, making it inaccessible to Small and Medium-sized Enterprises (SMEs) [7].

In Cameroon, existing machines are often unavailable, too expensive, energy-intensive, or unsuitable for SMEs. As a result, most restaurants still rely on inefficient manual methods. There is therefore a technological gap for a low-cost, locally manufactured, single motor machine capable of peeling and cutting potatoes simultaneously, while ensuring safety, efficiency, and maintainability.

To address this gap, the objective of this work is to design and develop a potato peeling and cutting machine that reduces processing time (less than 8 minutes for 7,000g of potatoes), minimizes physical effort, and achieves a peeling efficiency of at least 90%.

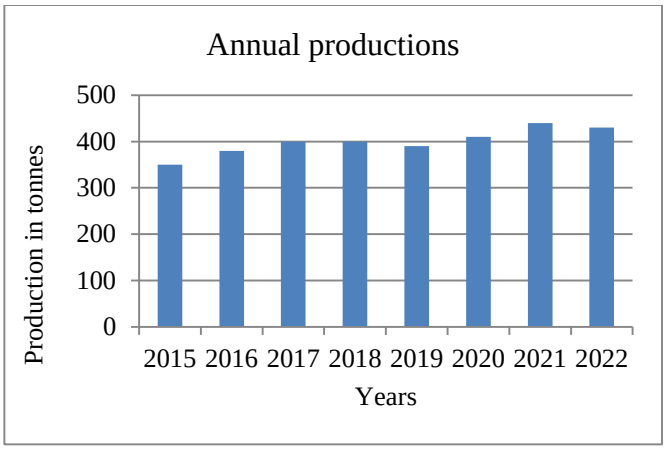

Fig. 1 Evolution of production (in tons) in Cameroon between 2015 and 2022 [8]

(a) (b) (c)

Fig. 2 Some potato peeling and cutting machines (a) Manual potato cutter, (b) Hand-cranked cutter, and (c) Potato peeler and cutter [7].

2. Materials and Methods

This section presents the materials and methods used for the design and construction of the potato peeler-cutter. Particular attention was paid to the capacity of the potato receiving pot, to the characteristics of all the components of the motion transmission chain, and to the computer-aided design software that allowed the creation of the mechanism drawings.

2.1. Machine Assessment Criteria

For an optimal choice, several criteria were used to assess the level of achievement of the objectives set at the start, and it was these criteria that were used to produce the kinematic diagram of the chosen solution. These criteria are as follows:

- Ability of the machine to perform the function of peeling and cutting potatoes optimally;
- Peeling and cutting performance;
- Hygiene conditions;
- Cost of the machine;
- Maintainability;
- Safety standards;
- Device size;
- Robustness.

2.2. Determination of Peeling and Cutting Efforts

Experimental studies on 10 potatoes have made it possible to determine the forces that the device will have to withstand in order to be able to carry out the required tasks.

Since the potatoes are assumed to be elliptical in shape, using a caliper (1) (Figure 3(a)), the major diameter ($D_{avg\ max}$) and minor diameter ($D_{avg\ min}$) *the radii* of the potato (2) were determined in order to evaluate the mean major radius and the mean minor radius, and to deduce the mean volume (V_{avg}) of a potato. Then, using a digital scale (3), the different masses (mi) of the potatoes (4) were determined to the hundredth of a gram, as shown in Figure 3(b). This then made it possible to obtain the mean mass (M_m) of a potato. The mean volume stated above made it possible to determine the total number (n) of potatoes that could be peeled simultaneously, knowing the volume V_E of the pot receiving the potatoes (10 l). This number made it possible to determine the total mass to be taken into account for peeling.

To determine the normal peeling force F_{EN}, an experiment was conducted as shown in Figure 3(c). This experiment mainly took into account the acceleration of gravity and the coefficient of friction $f = 0.8$ [9] of sandpaper. Sandpaper is the peeling tool chosen because of its abrasive properties.

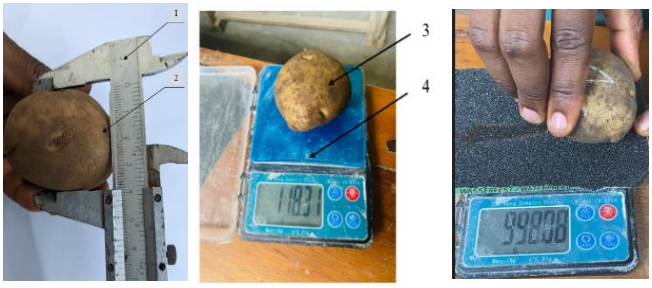

(a) (b) (c)

Fig. 3 Experimental device (a) Measurement of diameters; (b) Measurement of masses, and (c) Determination of peeling force.

The tangential force here is a function of the coefficient of friction f and the normal force F_{ET}. The following relations 1, 2, and 3 allowed us to find the normal force, the tangential force, and the peeling torque, respectively C_E.

$$F_{EN} = n.M_m.g \quad (1)$$

with $n = \frac{V_E}{V_{avg}}$ and $V_{avg} = \frac{4}{3}\pi.D_{avg\ max}.D_{avg\ min}{}^2$

$$F_{ET} = f.F_{EN} \quad (2)$$

$$C_E = D_E.F_T \quad (3)$$

Where D_E refers to the diameter of the pot in which the peeling is carried out.

Figure 4 (Machine available from the Civil Engineering Department of ENSET, Douala) shows the experimental device that allowed the determination of the normal compression force required for cutting. The potatoes are placed on the support (6) and held fixed by the fixed support (4). Using the lever (5), the operator exerts a compression force (3) on the potato. The deformation of the latter is measured using the digital comparator (2). The values obtained are then multiplied by a coefficient u = 329 in order to determine the compression forces F_D. The cutting torque is therefore given by relation 4.

$$C_D = D_D . F_D \quad (4)$$

Where D_D denotes the diameter of the crank.

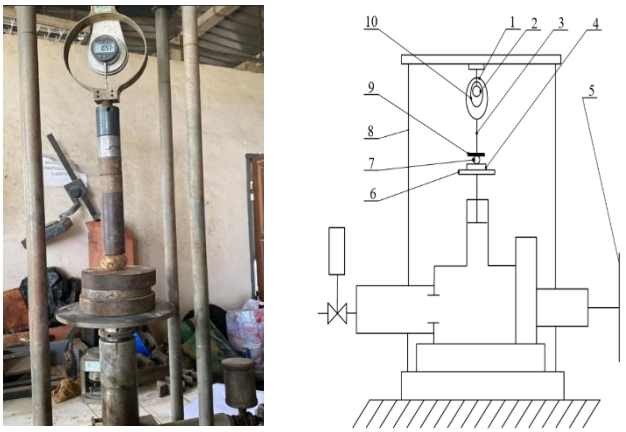

(a) **(b)**

Fig. 4 Experiment on compression force (a) Device, and (b) Kinematic diagram of the device.

2.3. Dimensional Study

The dimensions of the various elements of the machine were determined from experimental results as well as industrial norms and standards.

Power developed by the peeling system shaft (P_e) is a function of the peeling torque and is given by relation 5:

$$P_e = \frac{\pi N_e C_e}{30} \quad (5)$$

Where N_r denotes the desired rotation speed of the peeling shaft and $C_e$the peeling torque.

Power developed by the cutting system shaft P_d is a function of the cutting torque and is given by relation 6:

$$P_d = \frac{\pi N_d C_d}{30} \quad (6)$$

To obtain the engine power (P'_m), the overall efficiency of the transmission was taken into account.

2.3.1. Overall Performance

Power is transmitted to the shafts via the rolling bearings and the belt pulley system; hence, relation 7:

$$\eta = \eta_1 \times \eta_2 \quad (7)$$

Where η_1= 0.96 and η_2 =0.96, denotes the efficiencies of the belt pulley transmission and the rolling bearings, respectively [10].

2.3.2. Power Useful to the Engine

It is obtained using relation 8.

$$P'_m = \frac{P_e}{\eta} \quad (8)$$

The choice of engine here was made using the engine catalog [11].

To avoid having a rotation speed very far from the desired one, a reducer was associated with this motor in order to reduce the rotation speed of the drive pulley and to limit vibrations during operation.

2.4. Choice of Reducer

The reduction ratio i of the reducer is given by Equation (9).

$$i = \frac{N_m}{N_{rd}} \quad (9)$$

Where N_{rd} denotes the desired speed at the output of the reducer and N_m that of the motor, taking into account the desired rotation speed

2.5. Choosing Pulleys and Belts

The TEXROPE catalogue [10] was used for the selection of the elements of the pulley-belt system. Figure 5 illustrates how the pulley-belt transmission is carried out.

2.5.1. Terminology

d_p: Diameter of the receiving pulley;
Dp: Diameter of the drive pulley;
E: Center distance;
α_1: Winding angle on the small pulley;
α_2: Winding angle on the large pulley;
β: Tilt angle;
t: Tension of the slack strand;
T: Tension of the taut strand.

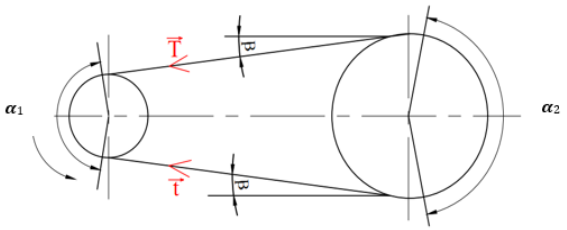

Fig. 5 Illustration of the transmission by pulley and belt system

2.5.2. Transmission Ratio

It was given by relation 10.

$$K = \frac{N_r}{N_{rd}} \quad (10)$$

Where N_r denotes the desired rotation speed at the output of the belt pulley system.

2.5.3. Pulley Diameters

Pulley diameters are determined using the relationship (11).

$$K = \frac{dp}{Dp}. \quad (11)$$

2.5.4. Linear belt speed

It was obtained by applying relation 12:

$$V = \frac{\pi d_p N_m}{60} \quad (12)$$

2.5.5. Theoretical Center Distance

According to relation 13, it should be understood in the interval:

$$0.5(d_p + \ ) + d_p \leq E \leq 3(\ D_p + d_p\ ) \quad (13)$$

2.5.6. Theoretical Belt Length

To find it, formula 14 was used:

$$L_{th} = 2E_{th} + 1{,}57(D_p + d_p) + \frac{(D_p - d_p)2}{4E_{th}} \quad (14)$$

2.5.7. Wrap Angle on the Small Pulley

We have the calculation using formula 15:

$$\alpha_1 = 180 - 2\sin^{-1}\frac{D_p - d_p}{2E_r} \quad (15)$$

2.5.8. Wrap Angle on the Large Pulley

We calculate it using formula 16:

$$\alpha_2 = 360 - \alpha_1 \quad (16)$$

2.5.9. Tilt Angle

We calculate it using formula 17:

$$\beta = 90° - \frac{\alpha_1}{2} \quad (17)$$

Slack strand tension and tight strand tension. They are determined by relations 18 and 19.

$$\begin{cases} T - t = \frac{60P_m}{\pi.d_p.N_m} & (18) \\ T = te^{3C_L f} & (19) \end{cases}$$

Depending on t the tension of the soft stand and T that of the tight stand, as well as C_L, the class of transmission.

2.6. Tree Sizing

Figures 6(a) and (b) represent the static models of the principal axes for the peeling system and the cutting system, respectively.

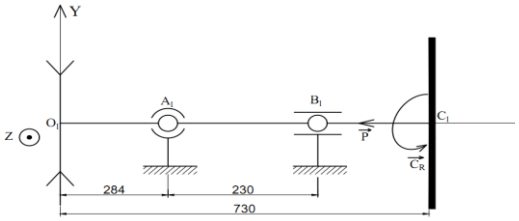

(a)

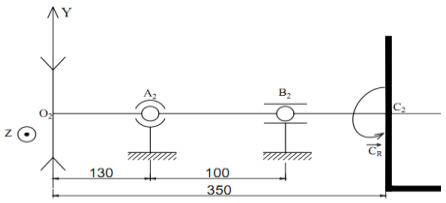

(b)

Fig. 6 Static modeling of the main axes (a) Peeling, and (b) Cutting.

From Figure 6, it can be seen that the parts mounted on the shafts cause various stresses. The dimensional study of these shafts allowed us to find diameters that will guarantee a reliable operation. In this sense, the application of the fundamental principle of statics allowed us to find the unknown forces, while the application of the resistance of materials allowed us to find the most stressed shaft sections, the types of stresses to which the shafts are subjected, and the minimum diameters.

The resistance conditions relating to the different stresses were studied by neglecting the shear stresses due to the shear forces and considering the stress concentration coefficient. Relation 20 represents the resistance criterion applied to the shaft of the peeling system, while relations 21 and 22 represent the Von Mises and Tresca criteria applied to the shaft of the cutting system.

$$\sqrt{(k_t\sigma)^2 + 3(k_t\tau)^2} \leq R_{Pe} \quad (20)$$

$$d \geq \sqrt[3]{\frac{32 \times s \times kt \times M_{if}}{\pi R_e}} \quad (21)$$

$$d \geq \sqrt[3]{\frac{16 \times s \times M_{it}}{\pi \times kt \times R_e}} \quad (22)$$

With k_t =1.4, the stress concentration coefficient, security coefficient s=3. The diameter values were also determined, taking into account the choice of the bearing. The bearings here were chosen using the calculation method of the industrial drawing memento Volume 2 [12], according to the assumption that the machine will be able to operate 10 hours per day for 10 years. In this case, the choice was made for single-row angular contact ball bearings.

2.7. Sizing of the Connecting Rod-Crank System

Connecting rod diameter d_B, The diameter of the crank is given by the relation 23:

$$d_B \geq \sqrt{\frac{4F_{N2}^2}{\pi\sigma}} \quad (23)$$

Connecting rod length L_B, Figure 7 shows connecting rod 1 at Top Dead Center (TDC) and Bottom Dead Center (BDC)

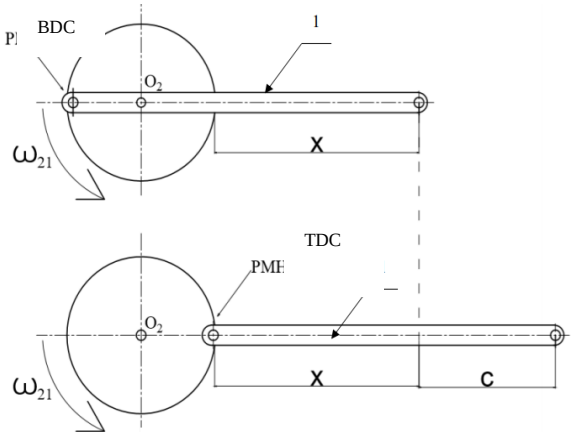

Fig. 7 Crank at BDC and TDC

The length of the connecting rod is given by relation 24.

$$L_B = x + c \quad (24)$$

With $c = D_D$; D_D being the radius of the crank.

2.8. Computer-Aided Design

This section presents the computer-aided design software that enabled the creation of the various drawings. Thus, the overall drawing and the kinematic diagram were designed using the AUTOCAD version 2016 software, while the 3D drawing of the prototype was designed using SOLIDWORKS version 2018 software. Figures 8(a) and 8(b) present the interfaces of the AUTOCAD 2016 and SOLIDWORKS 2018 software, respectively.

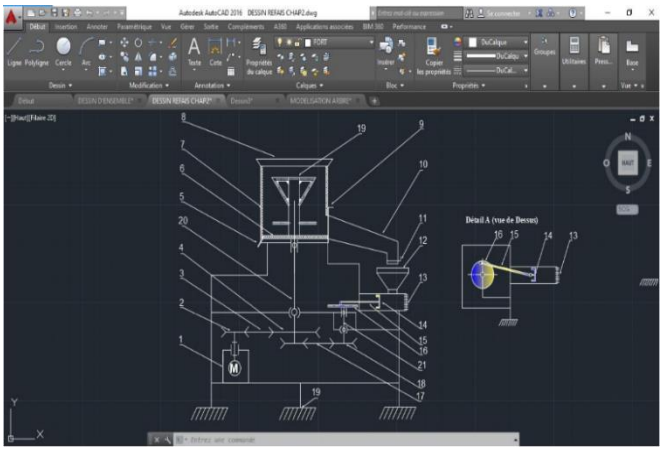

(a)

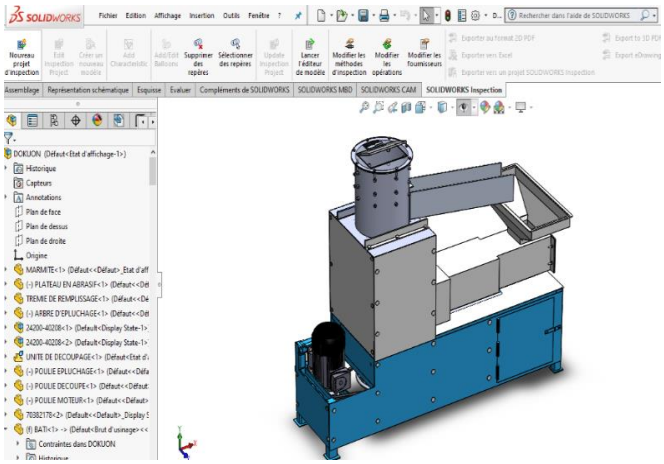

(b)

Fig. 8 Interface of the CAD software used (a) AUTOCAD 2016, and (b) SOLIDWORKS 2018.

3. Results and Discussion

This part is mainly dedicated to the processing and analysis of experimental and numerical results. It summarizes all the results obtained as well as the interpretations of these results.

3.1. Kinematic Diagram of the Mechanism

Figure 9 shows the kinematic diagram of the machine.

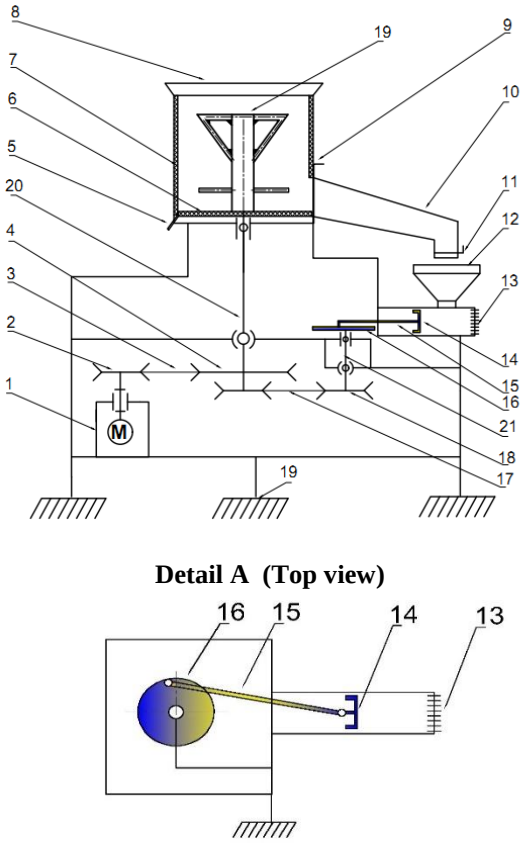

Fig. 9 Kinematic diagram of the mechanism

- Legend

1- Engine
2- Drive pulley
3- Transmission belt
4- Two-groove pulley
5- Waste outlet (water + peel)
6- Abrasive wheel
7- Fixed abrasive wall
8- Hopper
9-Trap
10-Peeled potato filling hopper
11-Trap
12-Hopper
13 - Blade plate; cutting
14 - Pusher
15 - Connecting rod
16 - Crank chainring
17 - Belt
18 - Receiving pulley
19- Blade
20- Main shaft
21 - Secondary shaft

- Description and Operation

The rotational movement of the motor is transmitted to the shaft 20 via the pulley-belt system (2 + 3 + 4). The rotation of this shaft rotates the plate 6, driving the potatoes, which then rub on the fixed abrasive walls 7, creating by friction, the peeling operation of the potatoes, favored by the introduction of water, which will come out with the peel (waste) through the orifice 5. Once the peeling operation is finished, the hatch 9 is opened, and the potatoes come out and are stored in the filling hopper in the form of a groove 10. When the hatch 11 is opened, the potatoes enter the cutting unit; they are expelled thanks to the blades 19. This operation is ensured by a connecting rod-crank system integral with the plate (16 + 17). The movement coming from the motor is transmitted to this system via the pulley-belt system (4 + 18 + 19). The connecting rod 16 transmits the transformed movement (rotational movement into translation) to the mobile pusher 15; this pushes the potatoes towards the fixed blade plate 14, which causes the cutting of the potatoes.

3.2. Characteristics of the Machine and Its Various Components

Table 1 presents the different results obtained. From the above, we note that the peeling and cutting torques have values of 59.07 Nm and 50.09 Nm, respectively, which implies that the shafts of the peeling system and the cutting system must develop powers of 623 W and 271 W. To meet these requirements, the motor must be able to develop a power of at least 663 W, which is why the LS 90L single-phase closed asynchronous motor with a power of 750 W and a rotation speed of 1500 rpm was chosen.

Since the shafts must not rotate at very high speeds, a WAF30 DT 80N4 reducer with a rater power of 750 *W* and a ratio of 6.57 was first coupled to the motor to also absorb the vibrations, then two belt pulley systems with a reduction ratio of 0.48 were then associated with this reducer in order to obtain the speeds required for the peeling and cutting operations. In addition, since the cutting must be done transversely, a crank rod system that was well dimensioned was coupled to the output of the cutting system shaft in order to transform the rotational movement into a translational movement. The diameter of the crank that describes the stroke of the connecting rod is therefore 74 mm, while the length of the connecting rod and its diameter have respective values of 35 mm and 274 mm.

Finally, the stress study revealed that the peeling system shaft is subjected to the composite stress of " bending + torsion + compression ", and that the cutting system shaft is subjected to the composite stress of " bending + torsion ". However, the stress study revealed that the shafts must have a minimum diameter of 27.8 mm and that the bearing range must be 40 mm, which is why the diameter chosen for both shafts is 50 mm. The shafts in question are supported by
SKF 7208 B angular contact bearings.

3.3. Computer-Aided Design

3D drawing: Figure 10 shows the 3D drawing of the machine created using SOLIDWORKS 2018 software.

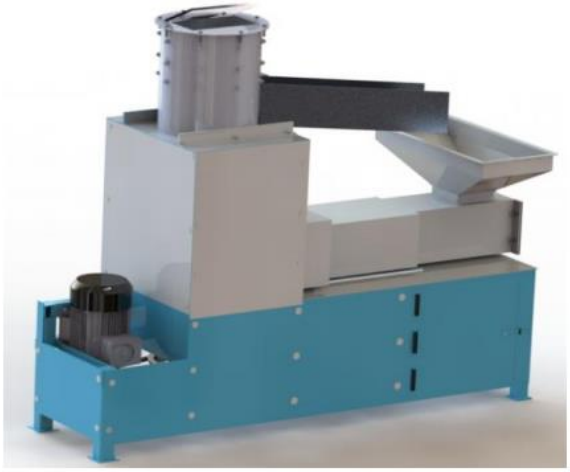

Fig. 10 3D drawing of the machine created using SOLIDWORKS 2018 software

3.4. Presentation of the Prototype

Figure 11 below shows the prototype produced (Figure11(a)); the peeled potatoes, as well as the cut potatoes (Figure 11(b)).

(a) **(b)**

Fig. 11 (a) Prototype produced, and (b) Peeled and cut potatoes.

From the previous images, we can see that the prototype is made entirely of stainless steel in order to comply with food safety standards. In addition, we also note that the system is completely dismountable and space-saving, which facilitates its maintenance.

3.4.1. Test Results

After 10 trials, the prototype could peel and cut an average of 7000g of potatoes in 7 minutes, and the peel was removed at 95%. This was largely satisfactory, because it corresponds to the minimum yield of 8 minutes for 7000g set in the objectives beforehand, with the removal of the peel at a level of more than 90% which was expected in the results.

3.5. Comparative Discussion

The performance of the developed potato peeling and cutting machine was compared with the semi-automatic prototype reported by reference [7]. Both studies share the objective of providing a low-cost solution for Small and Medium-sized Enterprises (SMEs), but they differ in design philosophy and operational performance.

Reference [7] reported a semi-automatic machine equipped with two separate motors: a 240 V AC motor for peeling and a 12V DC motor for cutting. Their prototype achieved a peeling efficiency of 98% and demonstrated a cutting speed of 0.64s per potato, which corresponded to an average improvement of 62% compared with manual cutting.

However, the system processed only about 3.08 kg of potatoes in 5 minutes (approximately 0.65kg/min) and relied on PVC brushes and mixed materials, which may limit durability and food safety compliance.

Table 1. Technical specifications of the potato peeling and cutting machine

Affected Components	Specification	Results
Engine	Peeling torque (C_E)	59.07 Nm
	Cutting torque (C_D)	50.09 Nm
	Power developed by the peeling system shaft (P_e)	623 W
	Power developed by the cutting system shaft(P_d)	271 W
	Power useful to the engine(P'_m)	663 W
	Power of the chosen engine(P_m)	750 W
	Rotation speed of the selected motor(V_m)	1500 rpm
	Designation of the chosen closed single-phase asynchronous motor	LS 90L [11]
Speed reducer	Required reduction ratio (i)	7
	Required torque (C_r)	30.17 Nm
	Power of the selected reducer (P_r)	750 W
	Designation of the selected reducer	WAF30 DT 80N4 [13]
Peeling system	Drive pulley diameter (d_{pe})	150 mm
	Diameter of the receiving pulley (D_{pe})	315 mm
	Designation of the chosen belt	SPZ 2360 [10]
	Actual center distance (a_e)	810.7 mm
	Designation of selected angular contact bearings	SKF 7208 B [12]
	Diameter chosen for the shaft (d_e)	50 mm
Cutting system	Drive pulley diameter (d_{pd})	95 mm
	Diameter of the receiving pulley (D_{pd})	200 mm
	Designation of the chosen belt	SPZ 1600 [10]
	Actual center distance (a_d)	566 mm
	Designation of selected angular contact bearings	SKF 7208 B [12]
	Diameter chosen for the shaft (d_d)	50 mm
Crank connecting rod system.	Crank diameter(D_D)	74 mm
	Connecting rod diameter(D_B)	35 mm
	Connecting rod length(L_B)	274 mm

In contrast, the present study introduces a more integrated design powered by a single 750W asynchronous motor coupled with a reducer and pulley-belt transmission system. This configuration allowed the prototype to process 7 kg of potatoes in 7 minutes (approximately 1kg/min), with peeling efficiency of 95% reported by reference [7]; the capacity and throughput were significantly higher. Furthermore, the use of stainless steel for all food-contact components enhances hygiene and durability, while the fully dismountable design ensures easier maintenance and cleaning. Overall, the proposed machine emphasizes energy efficiency, robustness, and scalability, whereas the Malaysian prototype mainly demonstrated functional feasibility and performance gains compared to manual methods. This comparison highlights the novelty of the present work, which lies in integrating both peeling and cutting into a single motor-driven system that balances efficiency, throughput, safety, and cost-effectiveness for SMEs in Cameroon.

4. Conclusion

This study presents a potato peeling and cutting machine integrating both functions into a single-motor system. Unlike existing devices, which are often too expensive or mainly designed for large-scale industrial use, the proposed prototype offers a locally adapted, low-cost, and efficient solution for Small and Medium-sized Enterprises (SMEs) in Cameroon. The machine demonstrated the ability to process 7 kg of potatoes in just 7 minutes, achieving a peeling efficiency of over 95%, which exceeds the performance objectives initially set. Beyond improving productivity and reducing physical effort, this innovation addresses a technological gap in the local agri-food sector by providing a safe, maintainable, and scalable tool. However, the water consumption during the peeling process was not fully considered, and future work should focus on optimizing the design to ensure resource efficiency for larger-scale applications. Overall, this machine represents a promising contribution to the modernization of potato processing in Cameroon and could support the growth of the local agri-food industry.

Acknowledgments

The authors would like to thank Prof. Fabien Betene Ebanda, Mr. Frank Loïc Gnintedem Zebaze, Mr. Cliff Orel Kuate Fono, Ms. Ingrid Bienvenue Onana, and Ms. Megane Doungmo Tchoffo for their valuable contributions and scientific input to this research work.

References

[1] John Ehiobu, Emrobowansan Idamokoro, and Anthony Afolayan, "Biofungicides for Improvement of Potato (Solanum tuberosum L) Production," *Scientifica*, vol. 2022, no. 1, 2022. [CrossRef] [Google Scholar] [Publisher Link]

[2] H. De Jong, "Impact of the Potato on Society," *American Journal of Potato Research*, vol. 93, pp. 415-429, 2016. [CrossRef] [Google Scholar] [Publisher Link]

[3] Christian Bachem et al., "Functional Genomic Analysis of Potato Tuber Life-Cycle," *Potato Research*, vol. 43, pp. 297-312, 2000. [CrossRef] [Google Scholar] [Publisher Link]

[4] Jean-Michel Lecerf, "Potato, A Valuable Tuber Vegetable," *Nutrition and Dietetics Notebooks*, vol. 45, no. 6, pp. S60-S67, 2010. [CrossRef] [Google Scholar] [Publisher Link]

[5] Ahmed Abbas et al., "An Artificial Intelligence Framework for Disease Detection in Potato Plants," *Engineering, Technology & Applied Science Research*, vol. 14, no. 1, pp. 12628-12635, 2024. [CrossRef] [Google Scholar] [Publisher Link]

[6] Olivier Arnaud Sadoung Noubossie, Guy Yakana Yombi, and Luther Ivan Fossi Tchiatagne, "*Diagnostic Report of the Potato Sector in Cameroon*," Project Financed by German Cooperation, 2023. [Google Scholar]

[7] Ahmad Faiz et al., "Semi-Automatic Potato Peeler and Cutter: An Initial Development," *Multidisciplinary Applied Research and Innovation*, vol. 2, no. 1, pp. 277-283, 2021. [Google Scholar] [Publisher Link]

[8] Dély Carlos Temfack Deloko et al., "Prevalence of Potato Viruses on Potato (Solanum Tuberosum L.) Grown in the Western Highlands of Cameroon," *Journal of Agriculture and Food Research*, vol. 5, pp. 1-6, 2021. [CrossRef] [Google Scholar] [Publisher Link]

[9] Richard T. Barrett, "*Fastener Design Manual*," NASA – RP-1228 Reference Publication, Report, pp. 1-100, 1990. [Google Scholar] [Publisher Link]

[10] TEXROPE Industrial Catalog, A Complete Range of Industrial Belts, 2008. [Online]. Available: https://www.actra.nl/wp-content/uploads/2014/09/593_TEXROPE_industrial_catalogue_English.pdf

[11] André Chevalier, Guide du Dessinateur Industrie, Pour Maîtriser la Communication Technique, HACHETTE Technique, 2004. [Online]. Available: https://www.academia.edu/41299043/Guide_du_dessinateur_industriel_chevalier

[12] Georges Lenormand, and Jacques Tinel, Industrial Drawing Handbook. Volume 2, Dimensional Documentation, Les Editions Foucher , Paris , 1987. [Online]. Available: https://search.worldcat.org/fr/title/37011357?oclcNum=37011357

[13] *Geared Motor Catalog*, SEW-EURODRIVE, pp. 1-147, 2015. [Online] Aailable: https://download.sew-eurodrive.com/download/pdf/20272545_G01.pdf

Appendix

Appendix 1: Nomenclature

REP	Nber	DESIGNATION	MATERIAL	OBSERVATION
59	01	Nut H M10	E300	Trade
58	02	Nut H M10	E300	Trade
57	02	Flat washer Type N 10,5-20	E300	Trade
56	01	Cover	Stainless steel	Mechanically welded
55	03	Screw S, M6-10	E300	Trade
54	01	Hinge	Stainless steel	Trade
53	02	Nut H M10	E300	Trade
52	02	Screw H M10	E300	Trade
51	02	Flat washer Type N 10,5-20	E300	Trade
50	01	Parallel key Type B 8×7×36	C30	Trade
49	01	Screw H, M10-45, 8.8	E300	Trade
48	01	Parallel key Type B 8×7×36	C60	Trade
47	01	Screw H, M10-45, 8.8	E300	Trade
46	04	Brackets	E300	Mechanically welded
45	02	Ball bearing 40 BC 33	100Cr7	Trade
44	01	Screw PY TL, M10-30	E300	Trade
43	02	Nut H M10	E300	Trade
42	02	Bushing	CuSn20	Trade
41	02	Circlip for bore 10×1	C60	Trade
40	02	Screw H, M10-50, 4.6	E300	Trade
39	01	Paulstra double lip seal	Rubber	Trade
38	32	Hatch	E300	Trade
37	01	Teflon	PTFE	Trade
36	04	Screw H, M10-45, 8.8	E300	Trade
35	04	Screw H, M6-18, 8.8	E300	Trade
34	01	Support	E300	Mechanically welded
33	02	Screw PY TL, M10-30	E300	Trade
32	01	Flat washer Type N 10,5-20	E300	Trade
31	08	Nut H M10	E300	Trade
30	04	Bearing block	E300	Trade
29	02	Ball bearing BE 40 BE 33	100Cr7	Trade
28	01	Parallel key Type A	C30	Trade
27	01	Flat washer Type N 10,5-20	E300	Trade
26	01	Screw H, M6-20, 8.8	E300	Trade
25	10	Nut H M6	E300	Trade
24	10	Screw H, M6-18, 4.6	E300	Trade
23	01	Cover	Polyester	Trade
22	01	Frame	S235	Mechanically welded
21	01	Cutting shaft	E300	Factory
20	01	Peeling shaft	E300	Factory
19	01	Scraper	Stainless steel	Mechanically welded
18	01	Receiver pulley ø 200	Alluminium	Trade
17	01	V-belt SPZ 9.7×8×2360	Rubber	Trade
16	01	Crank	E300	Trade
15	01	Connecting rod	E300	Trade
14	01	Pusher	Stainless steel	Mechanically welded
13	01	Blade plate	Stainless steel	Mechanically welded
12	01	Cutting hopper	Stainless steel	Mechanically welded
11	01	Hatch	Stainless steel	Mechanically welded
10	01	Guide	Stainless steel	Mechanically welded
9	01	Evacuation hatch	Stainless steel	Mechanically welded
8	01	Pot	Stainless steel	Mechanically welded
7	01	Abrasive	Ceramic AL_2O_3	Trade
6	01	Plate	Stainless steel	Trade
5	01	Spacer	E300	Mechanically welded
4	01	Two-groove pulley ø 315-95	Alluminium	Trade
3	01	V-belt SPZ 9.7×8×2360	Rubber	Mechanically welded
2	01	Driving pulley ø 150	Alluminium	Trade
1	01	Motor		Trade

SCALE 1:4

OVERALL DRAWING OF THE POTATO PEELING AND CUTTING MACHINE

Appendix 2: General assembly drawing